Weierstraß-Institut
für Angewandte Analysis und Stochastik

Stripe-array diode-laser in an off-axis external cavity: Theory and experiment

Andreas Jechow [1], Mark Lichtner [2], Ralf Menzel [1], Mindaugas

Radziunas [2], Danilo Skoczowsky [1] and Andrei G. Vladimirov [2]

submitted: 25th September 2009

[1] University of Potsdam,
    Institute for Physics and Astronomy
    Chair of Photonics
    Karl-Liebknecht-Str. 24-25
    14476 Potsdam
    E-Mail: ajechow@uni-potsdam.de
    ralf.menzel@physik.uni-potsdam.de
    skoczows@rz.uni-potsdam.de

[2] Weierstrass Institute for Applied
    Analysis and Stochastics
    Laser-Dynamics Group
    Mohrenstrasse 39
    D - 10117 Berlin
    Germany
    E-Mail: lichtner@wias-berlin.de
    radziunas@wias-berlin.de
    vladimir@wias-berlin.de

W I A S

Abstract

Stripe-array diode lasers naturally operate in an anti-phase supermode. This produces a sharp double lobe far field at angles $\pm\alpha$ depending on the period of the array. In this paper a 40 emitter gain guided stripe-array laterally coupled by off-axis filtered feedback is investigated experimentally and numerically. We predict theoretically and confirm experimentally that at doubled feedback angle 2α a stable higher order supermode exists with twice the number of emitters per array period. The theoretical model is based on time domain traveling wave equations for optical fields coupled to the carrier density equation taking into account diffusion of carriers. Feedback from the external reflector is modeled using Fresnel integration.

1 Introduction

High power broad area diode lasers (BALs) reach electro-optical efficiencies of more than 70% [1] and can exhibit output powers of more than 20 W [2] as single emitters and several hundred Watts when they are combined in laser bars [3]. The main drawbacks of BALs are poor spatial beam quality in the lateral direction and longitudinal multimode operation. Several techniques for improving the spatial beam quality of BALs and laser bars exist. This includes the use of phase masks [4], phase conjugation [5] and off-axis feedback [6, 7, 8, 9, 10]. Laterally coupled stripe-arrays have a similar emitting area as BALs. These devices typically operate in a supermode, where each stripe corresponds to a single laser emitter and neighboring emitters are coupled anti-phase. This anti-phase supermode can be stabilized by off-axis feedback [11, 12].

In this work, we investigate numerically and experimentally a 40 emitter stripe-array with an off-axis filtered feedback. We extend the dynamic 2+1-dimensional traveling wave BAL model [13] by including a filtered off-axis feedback, which is calculated using Fresnel integration. We have verified our model by comparing the simulation results to the previously reported experimental data [14] on anti-phase operation at the feedback angle $\alpha_{FB} = \lambda_0/(2d)$, where λ_0 is the central wavelength and d is the stripe pitch. At twice larger feedback angle λ_0/d our simulations predict a field emission with the lateral mode characterized by a pair of anti-phase near field intensity peaks per stripe pitch. In this regime, due to strong global coupling, the array has double the number of emitters than stripes. Experimental evidence supporting this theoretical prediction is given.
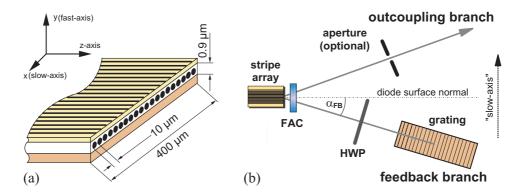
1

Figure 1: 40 emitter stripe-array (a) and setup of the off-axis ECDL in the slow-axis plane (b).

2 Experimental setup

The stripe-array used in this work is depicted in Fig. 1 (a). The emitter had a width of $w = 400$ μm and the chip length was $l = 1500$ μm. 40 contact stripes each with a width of $w_{stripe} = 4$ μm and a pitch of $d = 10$ μm were realized by etching trenches with a depth of 200 nm into the p-doped cap layer before metalization. The active region consisted of a 7 nm thick InGaAs quantum well embedded in a 880 nm thick AlGaAs core region [15]. To be operated in an external cavity diode laser (ECDL) the front facet was AR coated with $R_0 \approx 4 \cdot 10^{-4}$, while the back facet had $R_{-l} > 90$ %. This device yielded more than 6 W of output power when operated in an on-axis ECDL [16], but with a lateral beam quality of $M^2 \approx 35$, only.

The experimental setup of the off-axis ECDL is depicted in Fig. 1 (b) and is described in more detail in Ref. [14]. The cavity consisted of only four optical components: the stripe-array, a fast axis collimator (FAC), a half wave-plate (HWP) and a holographic reflective diffraction grating (g = 1800 lines/mm). In direction of the fast-axis, a Littrow type feedback was realized. In slow-axis direction, the grating possessed no wavelength selectivity. It was used to select the feedback angle. By stabilizing the anti-phase supermode, more than 1 W of diffraction limited, tunable light could be achieved [14].

3 Mathematical model

To simulate the dynamics of the stripe-array we use the 2+1 dimensional traveling wave (TW) model discussed in details in Ref. [13]. According to this model the spatio-temporal evolution of slowly varying complex amplitudes $\psi^{\pm}(t, z, x)$ of two counterpropagating waves is governed by the TW equations

$$\partial_t \psi^{\pm} + \frac{i v_g}{2 k_0 \overline{n}} \partial_{xx} \psi^{\pm} = v_g \left[\mp \partial_z - i \beta(z, x) \right] \psi^{\pm} + F_{sp}^{\pm}, \quad -l < z < 0, \quad -\frac{w}{2} < x < \frac{w}{2},$$

2

where v_g, $k_0 = 2\pi/\lambda_0$, $\overline{n}$, and $F_{sp}^{\pm}$ are the group velocity of light, the free-space central wavenumber, the reference refractive index, and the Langevine noise term, respectively. l is the chip length and w is the lateral width of the stripe-array. The complex propagation factor β describes linear loss, gain, and refractive index in the semiconductor material. This factor depends on the excess carrier density and takes into account the refractive index change due to Joulean heating. The equation for the carrier density contains a term describing carrier diffusion in the direction x. The wavelength dependence of the material gain is described by an additional linear equation which introduces Lorentzian spectral filtering. The variation of the injection current in x- direction is approximated by a peace-wise constant function. For a full description of parameters used in simulations we refer to [13].

The amplitudes $\psi^{\pm}$ satisfy the following boundary conditions:

$$\psi^+(t, -l, x) = \sqrt{R_{-l}}\psi^-(t, -l, x), \ \ \psi^-(t, 0, x) = \sqrt{R_0}\psi^+(t, 0, x) + (1 - R_0)\mathcal{F}\psi_{FB}(t, x),$$

at the laser facets $z = -l$ and $z = 0$. Here, $R_{-l} = 0.9$ and $R_0 = 4 \cdot 10^{-4}$ are the reflectivities of these facets. The linear operator $\mathcal{F}$ accounts for the spectral filtering performed by the grating. It is modeled by a Gaussian filter with the full width at half maximum of $\sim 0.1nm$. Such a narrow spectral filter is required to obtain a stable single compound cavity mode cw operation. Replacing the feedback mirror by an infinite reflecting plane located at a distance $D = 3.9cm$ from the right facet and tilted by the angle α_{FB}, we express the optical field $\psi_{FB}(t, x)$ reinjected into the chip by means of the Fresnel integral:

$$\psi_{FB}(t, x) = \sqrt{\frac{1}{i\lambda_0 2D}} \int_{-w/2}^{w/2} \psi^+ \left(t - \frac{2D}{c_0}, 0, x'\right) e^{-ik_0 \text{dist}(x', x)} \, dx'.$$

Here $\text{dist}(x', x)$ denotes the shortest distance between two lateral points x' and x at the output facet of the array which the light takes to travel via the reflection from the external plane.

4 Discussion of numerical and experimental results

Near- and far field distributions of the stripe-array at off-axis feedback angles $\alpha_{FB} = \lambda_0/(2d) \approx 2.8°$ and $\alpha_{FB} = \lambda_0/d \approx 5.6°$ have been measured and calculated numerically. Experimental results are depicted in Fig. 2 and the theoretical simulations are shown in Fig. 3. The lefthand side in these figures show the results for a feedback angle of $\alpha_{FB} = 2.8°$, the righthand side the results for $\alpha_{FB} = 5.6°$, respectively. The far fields (a, b in the figures) exhibit two asymmetric lobes at the angles $\pm\alpha_{FB}$. In qualitative agreement with the measurements, the simulations show a strong output lobe and a reduced feedback lobe at the location of the mirror $(+\alpha_{FB})$, which is usual when asymmetric feedback is applied [7, 8].

Measured near fields are shown in Fig. 2 (c, d), calculated near fields and phases are shown in Fig. 3 (c-f). The two lower graphs (e, f) show zoomed near fields of three stripes. In these graphs the area where the carriers are injected through is indicated by the grey vertical stripes.

For $\alpha_{FB} = 2.8°$, the near field has ≈ 40 maxima with nearly flat peak intensity distribution as can be seen in panels c) in Figs. 2 and 3. As expected, the positions of these maxima correspond to the contact stripes, see panel e) of Fig. 3. As it is known from previous studies, the stripe-array operates stable in the anti-phase regime when the feedback angle is close to $\alpha_{FB} = \lambda_0/(2d)$. The near field phase is shown by black bullets in Fig. 3 (c,e), where the π phase shift between emitters and the corresponding stripes can be seen. This supermode is stabilized with the external cavity, because the phase difference of the optical fields reinjected into the neighboring stripes of the amplifier (i.e., at the positions x and $x \pm d$) is $d2\pi \sin \alpha_{FB}/\lambda_0 \approx \pi$.

The phase of the reinjected field is shown by gray bullets in Fig. 3 (c,e). Since neighboring emitters are synchronized in anti-phase the feedback becomes maximal and a plane wave resonator is established [17]. Thus, the (native) antiphase coupling between neighboring stripes is supported by the external feedback and the laser operates at maximal output power ($> 1W$) in a stable anti-phase supermode.

For $\alpha_{FB} = 5.6°$, the distribution of the maxima in the near field becomes strongly inhomogeneous. The calculated near fields presented in panels e,f) of Fig. 3 indicate that the number of field maxima is doubled. This may be understood by assuming that each stripe locally operates in its second transverse mode. By doubling the feedback angle to $\alpha_{FB} = 5.6°$, the feedback phase rotates approximately twice as fast when moving along the lateral x axis, see gray bullets in Fig. 3 (d,f). In this case two lateral positions x and $x \pm d$ are connected in-phase by the feedback field, while x and $x \pm d/2$ are coupled anti-phase. Hence a supermode with about a doubled number of near field maxima becomes stable.

It is seen from Fig. 3 (d,f) that this higher supermode can be considered to consist of ~ 40 second order modes of individual stripes coupled to each other. Similarly to the lowest order anti-phase supermode this higher order supermode maximizes the feedback and establishes a plane wave resonator [17]. However, since the distance between the anti-phase near field maxima is halved, the angle of the far field peaks is doubled.

Figure 4 shows a full spatial plot of the calculated higher order supermode. Since the distance between the near field maxima are narrowed, the portion of the area occupied by the emitters divided by the total area of the stripes is reduced. Hence, the conversion of carriers into photons through stimulated recombination is also reduced. Correspondingly, in simulations we have observed an optical power drop off of about 50%.
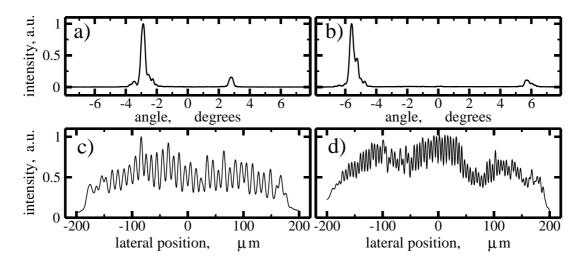
4

Figure 2: Measured far fields (a,b) and near fields (c,d) for $\alpha_{FB} = 2.8°$ (a,c) and $\alpha_{FB} = 5.6°$ (b,d).
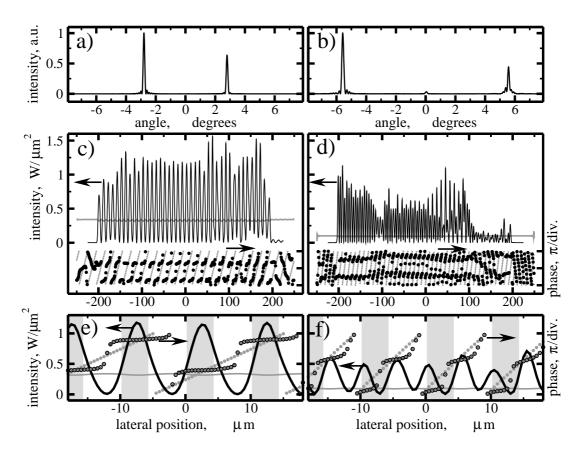

Figure 3: Calculated far fields (a,b), full (c,d) and zoomed (e,f) near field intensity (black curves) and phase (black bullets) for $\alpha_{FB} = 2.8°$ (a,c,e) and $\alpha_{FB} = 2.6°$ (b,d,f). The location of the contact stripes are indicated by the shaded vertical bars in the zoomed near fields (e,f). Grey lines and bullets in (c,d,e,f) represent intensity and phase of the reinjected field.
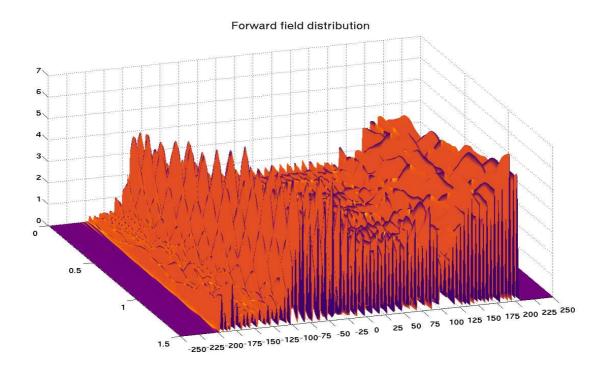
Figure 4: Calculated forward field intensity for the supermode at $\alpha_{FB} = 5.6°$.

5 Conclusion

We have performed a numerical and experimental study of a multistripe diode laser array with strong global coupling between the stripes via off-axis optical feedback. Stable anti-phase synchronization of individual stripes can be achieved by adjusting the feedback angle to $\alpha_{FB} \approx \lambda_0/2d$, where d is the stripe pitch. This angle corresponds to a feedback phase difference of $\sim \pi$ between neighboring stripes. Numerical results for this regime, which correspond to the lowest order lateral anti-phase supermode, are in agreement with the experimental data. Furthermore, we have predicted theoretically and verified experimentally that at twice larger feedback angle $\alpha_{FB} \approx \lambda_0/d$ a higher order stable lateral supermode exists with twice the number of emitters per period d. In this regime the feedback phase between neighboring stripes rotates by $\sim 2\pi$. Thus there exist two anti-phase emitters within the lateral distance d which collectively form a plane wave resonator at doubled angle.

Previous theoretical studies of globally coupled laser arrays were mainly concentrated on investigation of in-phase and anti-phase synchronization between the lasers resulting from on-axis feedback (see e.g. [18]). Numerical investigation of synchronization of a diode laser array close to threshold by angular optical injection was performed in [17]. However, up to our knowledge, a comprehensive time domain numerical modeling of the high power behavior of stripe-arrays taking into account off-axis filtered optical feedback, diffraction, lateral coupling between the stripes via overlapping fields, and carrier diffusion, has not been performed before.

Thus, for the first time self consistent dynamic modeling of an external cavity com-

prising an array of coupled diode lasers is presented.

Acknowledgements

References

[1] M. Kanskar, T. Earles, T.J. Goodnough, E. Stiers, D. Botez, and L.J. Mawst, "73% CW power conversion efficiency at 50 W from 970 nm diode laser bars," Electron. Lett. **41**, 245 – 247 (2005).

[2] K. J. Paschke, S. Einfeldt, A. Ginolas, K. Häusler, P. Ressel, B. Sumpf, H. Wenzel, and G. Erbert, "15 - W Reliable Operation of 96 - μm Aperture Broad-Area Diode Lasers Emitting at 980 nm," in CLEO/QELS 2008 Conference Digest p. CMN4 (2008).

[3] H. Li, I. Chyr, X. Jin, F. Reinhardt, T. Towe, D. Brown, T. Nguyen, M. Berube, T. Truchan, D. Hu, R. Miller, R. Srinivasan, T. Crum, E. Wolak, R. Bullock, J. Mott, and J. Harrison, ">700W continuous-wave output power from single laser diode bar," Electron. Lett. **43**, 27–28 (2007).

[4] N. Stelmakh, "Harnessing Multimode Broad-Area Laser-Diode Emission Into a Single-Lobe Diffraction- Limited Spot," IEEE Photon. Tech. Lett. **19**, 1392–1394 (2007).

[5] K. Iida, H. Horiuchi, O. Matoba, T. Omatsu, T. Shimura, and K. Kuroda, "Injection locking of a broad-area diode laser through a double phase-conjugate mirror," Opt. Commun. **146**, 6–10 (1998).

[6] S. Wolff, A. Rodionov, V. Sherstobitov, and H. Fouckhardt, "Fourier-optical transverse mode selection in external-cavity broad-area lasers: experimental and numerical results," IEEE J. Quantum Electron. **39**, 448–458 (2003).

[7] L. Lang, J. J. Lim, S. Sujecki, and E. C. Larkins, "Improvement of the beam quality of a broad-area diode laser using asymmetric feedback from an external cavity," Opt. Quantum Electron. (2009).

[8] M. Chi, B. Thestrup, and P. M. Petersen, "Self-injection locking of an extraordinarily wide broad-area diode laser with a 1000-μm-wide emitter," Opt. Lett. **30**, 1147–1149 (2005).

[9] A. Jechow, V. Raab, and R. Menzel, "High cw power using an external cavity for spectral beam combining of diode laser-bar emission," Appl. Opt. **45**, 3545 – 3547 (2006).

[10] D. Vijayakumar, O. B. Jensen, and B. Thestrup, "980 nm high brightness external cavity broad area diode laser bar," Opt. Express **17**, 5684–5690 (2009).

[11] C. J. Chang-Hasnain, J. Berger, D. R. Scifres, W. Streifer, J. R. Whinnery, and A. Dienes, "High power with high efficiency in a narrow single-lobed beam from a diode laser array in an external cavity," Appl.Phys. Lett. **50**, 1465–1467 (1987).

[12] L. Goldberg and J. Weller, "Narrow lobe emission of high power broad stripe laser in external resonator cavity," Electron. Lett. **25**, 112–114 (1989).

[13] M. Spreemann, M. Lichtner, M. Radziunas, U. Bandelow, and H. Wenzel, "Measurement and Simulation of Distributed-Feedback Tapered Master-Oscillator Power Amplifiers," IEEE J. Quantum. Electron. **45**(6), 609–616 (2009).

[14] A. Jechow, V. Raab, R. Menzel, M. Cenkier, S. Stry, and J. Sacher, "1 W tunable near diffraction limited light from a broad area diode in an external cavity with a line width of 1.7 MHz," Opt. Commun. **277**, 161 – 165 (2007).

[15] M. Mikulla, P. Chazan, A. Schmitt, S. Morgott, A. Wetzel, M. Walther, R. Kiefer, W. Pletschen, J. Braunstein, and G. Weimann, "High-brightness tapered semiconductor laser oscillators and amplifiers with low-modal gain epilayer-structures," IEEE Photon. Techn. Lett. **10**, 654–656 (1998).

[16] A. Jechow, V. Raab, and R. Menzel, "Tunable 6.8 W narrow bandwidth emission from a single-stripe continuous-wave broad-area laser diode in a simple external cavity," Appl. Opt. **47**, 1447 – 1450 (2008).

[17] G. R. Hadley, A. Owyoung, and J. P. Hohimer, "Modeling of injection-locking phenomena in diode-laser arrays," Optics Letters **11**(3), 144–146 (1986).

[18] G. Kozyreff, A. G. Vladimirov, and P. Mandel, "Global coupling with time delay in an array of semiconductor lasers," Phys. Rev. Lett. **85**(18), 38093812 (2000).